Performance of some nucleation theories with a nonsharp droplet-vapor interface

Ismo Napari,[a] Jan Julin, and Hanna Vehkamäki
Department of Physics, P.O. Box 64, University of Helsinki, Helsinki 00014, Finland

(Received 30 June 2010; accepted 24 September 2010; published online 15 October 2010)

Nucleation theories involving the concept of nonsharp boundary between the droplet and vapor are compared to recent molecular dynamics (MD) simulation data of Lennard-Jones vapors at temperatures above the triple point. The theories are diffuse interface theory (DIT), extended modified liquid drop-dynamical nucleation theory (EMLD-DNT), square gradient theory (SGT), and density functional theory (DFT). Particular attention is paid to thermodynamic consistency in the comparison: the applied theories either use or, with a proper parameter adjustment, result in the same values of equilibrium vapor pressure, bulk liquid density, and surface tension as the MD simulations. Realistic pressure-density correlations are also used. The best agreement between the simulated nucleation rates and calculations is obtained from DFT, SGT, and EMLD-DNT, all of which, in the studied temperature range, show deviations of less than one order of magnitude in the nucleation rate. DIT underestimates the nucleation rate by up to two orders of magnitude. DFT and SGT give the best estimate of the molecular content of the critical nuclei. Overall, at the vapor conditions of this study, all the investigated theories perform better than classical nucleation theory in predicting nucleation rates. © *2010 American Institute of Physics*. [doi:10.1063/1.3502643]

I. INTRODUCTION

Classical nucleation theory (CNT)[1,2] has been a mainstay of atmospheric nucleation studies and technological applications for decades. CNT offers mathematical simplicity and very little computational challenge, but it gives poor performance in many cases.[3] Many new theoretical approaches have been invented during the recent decades in attempts to surpass and replace CNT but the success of these theories has been limited. For example, they may fail in some ambient conditions, they can only be applied to a certain class of substances, or they require data that are not easily available. The quality and limitations of the theories can only be assessed by comparing them to experiments; however, in some cases the observed nucleation rates are found to depend on the experimental method[4] and the approximations when data is analyzed.[5]

In this paper, we try to circumvent the issues concerning the experimental uncertainties by comparing nucleation theories to recent molecular dynamics (MD) simulations, where the condition of the nucleating vapor is controlled more easily and exactly than in experiments. For example, in MD, the nucleating vapor can be connected directly to an artificial thermostat for a stricter regulation of temperature than could be achieved experimentally by a carrier gas. The nucleation rate is also accurately obtained by following the formation and growth of the clusters in the vapor, a task that is, in practice, impossible in an experiment. MD is unfortunately computationally demanding and in most of the nucleation studies by MD, simple Lennard-Jones (LJ) systems have been investigated. For the purpose of this study, we have chosen very recent sets of MD nucleation data in LJ systems.[6–8] Nucleation of molecular substances might present a more stringent test of a theory, but lacking MD data at various temperatures and vapor conditions, such a study is not possible at the moment.

The investigated nucleation theories are diffuse interface theory (DIT),[9] extended modified liquid drop model combined with dynamical nucleation theory (EMLD-DNT),[10,11] square gradient theory (SGT),[12,13] and density functional theory (DFT).[14] These theories are connected by the fact that they incorporate, explicitly or implicitly, a nonsharp boundary between the nucleating cluster and the vapor. There are, however, differences in the input data needed to apply these theories to nucleation. DIT requires the heat of evaporation in addition to the same set of thermophysical quantities as CNT. If the vapor can be considered ideal, the same quantities as in CNT are all that is needed to apply EMLD-DNT. However, in the case of a nonideal vapor, EMLD-DNT also requires an equation of state (EoS) for the vapor. SGT must always be supplemented with a complete EoS and DFT needs the exact molecular interaction potential. A short review of the theories is presented in Sec. II.

We aim to attain internal consistency to the comparison between theory and simulation by using the MD values for certain thermodynamic bulk properties in the theories. In some cases, this is achieved by a fitting procedure, as explained in Sec. III in more detail. The thermodynamic consistency at the bulk level will help in revealing the true differences between the theories when compared to the MD nucleation simulations. Thus, although the applied theories are all well known and they do not contain any new features, a better insight to the validity of the theories will be found.

Our work parallels to that by Kalikmanov *et al.*,[15] where

[a]Electronic mail: ismo.napari@helsinki.fi.

several theoretical approaches to nucleation were compared to MD simulations of LJ vapors. However, all the investigated theories in our work are not the same as in Ref. 15 and different sets of MD simulations are used as references. A further noteworthy difference between Ref. 15 and our work is the temperature range: in Ref. 15, nucleation was mainly studied below the triple point, whereas we consider temperatures above it. This ensures that the critical droplets are liquidlike. The high temperatures necessitate the use of a realistic EoS instead of ideal gas law because MD simulations are restricted to fairly high vapor saturation ratios, where significant departure from ideal gas is observed especially above triple point (see Sec. III).

The objective of this work is to determine which of the theories listed above is the best in reproducing the nucleation properties observed in MD simulations of LJ fluid. We are mainly interested in the key observable quantity in nucleation, the nucleation rate (Sec. IV A). Nevertheless, using the nucleation rate data, we also evaluate the critical cluster sizes and compare them to the cluster sizes obtained from the investigated theories (Sec. IV B). This study thus also constitutes a follow-up of our previous work,[7] where cluster sizes in MD simulations were compared according to various cluster definitions. Finally, in Sec. IV C, we discuss the effect of EoS on the theoretical nucleation rates and cluster sizes and in Sec. V we present our conclusions.

II. A SHORT REVIEW OF THE THEORIES

A. DIT

Diffuse interface theory[9] is based on a parametrization of radial enthalpy $\Delta h(r)$ and entropy $\Delta s(r)$ profiles of the droplet. The work of formation of the droplet (that is, the grand potential difference $\Delta\Omega$ in an open system) can be expressed in terms of step profiles $\Delta h(0)$ and $\Delta s(0)$ as

$$\Delta\Omega = \frac{4\pi}{3}(R_H^3\Delta h(0) - R_S^3 T\Delta s(0)), \tag{1}$$

where R_H and R_S are the respective positions of the steps and $R_H = R_S - \delta$, where δ is the interfacial thickness. If the bulk properties are assumed to prevail at least at the center of the droplet, $\Delta h(0)$ and $\Delta s(0)$ can be replaced by their bulk liquid values Δh and Δs. Furthermore, if δ is assumed independent of saturation ratio at fixed temperature, one can estimate $\delta = -\gamma_\infty/\Delta h_f$, where γ_∞ is the surface tension of the planar interface and Δh_f is the volumetric heat of fusion.

The work of formation of the critical cluster is found from the maximum of $\Delta\Omega$. With the above assumptions, the maximum of Eq. (1) is given by

$$\Delta\Omega^* = -\frac{4\pi}{3}\delta^3\Delta g\psi, \tag{2}$$

where $\Delta g = \Delta h - T\Delta s$, $\psi = 2(1+q)\eta^{-3} - (3+2q)\eta^{-2} + \eta^{-1}$, $q = (1-\eta)^{1/2}$, and $\eta = \Delta g/\Delta h$. The Gibbs free energy density difference Δg is obtained from $\Delta g = -\rho_l\Delta\mu$, where $\Delta\mu$ is the chemical potential difference between supersaturated and saturated vapor and ρ_l is the bulk liquid density.

Compared to CNT, DIT has been shown to give improved predictions of nucleation rates of nonpolar, weakly polar, and metallic substances.[9] For polar substances (such as water), the theory is less successful.

B. EMLD-DNT

The extended liquid drop model combined with the dynamical nucleation theory[10,11] is in principle an extension of CNT, but it has many features which makes it a more realistic theory than CNT. EMLD-DNT is formulated for a system of N molecules in a spherical container of volume V (so-called N,V-cluster). The container encloses a liquid drop of n molecules and $N-n$ vapor molecules. The Helmholtz free energy differential for such a system is written as[16]

$$(dF)_{N,V,T} = -\left(P_l - P_v - \frac{2\gamma_\infty}{r}\right)dV_l + (\mu_l - \mu_v)dn, \tag{3}$$

where P_l and P_v are the pressures inside the drop and in the vapor, μ_l and μ_v are the corresponding chemical potentials, V_l is volume of the drop, and r is the radius of the drop. Assuming incompressible liquid Eq. (3) can be integrated to give the formation energy in the closed container

$$\Delta F(n) = F(n) - F(0) = \int_0^n (P_v - P_e)v_l dn' - \int_0^n (\mu_v - \mu_e)dn' + \gamma_\infty A(n), \tag{4}$$

where P_v and μ_v are the pressure and the chemical potential at the density $(N-n)/(V-nv_l)$, P_e is the pressure of saturated vapor, $v_l = 1/\rho_l$ is the molecular volume in the liquid, and A is the surface area of the cluster.

The essential idea in the EMLD model is the fluctuation of cluster size.[16] The drop size does not have a fixed value inside the container but instead it fluctuates with the relative probability of a fluctuation of size n given by $f(n) \propto \exp(-\Delta F(n)/k_BT)$. Knowing the free energies $\Delta F(n)$ for all $n = 0,\ldots,N$, the canonical partition function $Z(N,V,T) = -k_BT\ln(\Sigma_{n=0}^N \exp(\Delta F(n)/k_BT))$ and the free energy difference $\Delta F = -k_BT\ln Z$ can be calculated.

Another important essence of the EMLD model is the incorporation of the dynamical nucleation theory, which together with the variational transition state theory gives a unique cluster definition: the volume V of the N,V-cluster is such that the evaporation rate is minimized. This condition amounts to finding the volume which minimizes the vapor pressure in the container. Note that due to the fluctuating cluster size, the pressure must be calculated as an ensemble average. Furthermore, since the cluster (considered as a single hard-sphere particle) is free to move inside container, a translation correction must be added to the pressure.[16]

Once the minimum pressure $P_{\min}$ and the corresponding volume $V_{\min}$ are found for a given critical size N^*, the formation free energy of the cluster in the vapor at pressure $P^* = P_{\min}$ is obtained from[11]

$$\Delta\Omega^* = \Delta F(N^*, V_{\min}) - V_{\min}(P_0 - P^*) + N^*\Delta\mu_0^*, \tag{5}$$

where $P_0 = P(\rho_0)$, $\Delta\mu_0^* = \mu(P_0) - \mu(P_{\min})$, and $\rho_0 = N/V_{\min}$.

Note that although EMLD-DNT uses the concept of classical drop with a sharp boundary, the translating drop and its fluctuating size produces an averaged density profile.[17]

EMLD-DNT has been shown to be in a very good agreement with Monte Carlo simulation,[11] MD simulation,[18] and 1-pentanol data[19] on nucleation.

C. SGT

In the square gradient theory, the free energy of cluster in a vapor characterized by chemical potential μ is given by[12,13,20]

$$\Omega[\rho(\mathbf{r})] = \int \left\{ f_0(\rho(\mathbf{r})) + \frac{c}{2}[\nabla\rho(\mathbf{r})]^2 - \mu\rho(\mathbf{r}) \right\} d\mathbf{r}, \tag{6}$$

where $f_0(\rho)$ is the local free energy density of the uniform fluid and c is a (temperature-dependent) constant. The salient feature of SGT is the dependence of the free energy on slope of the density profile $\rho(\mathbf{r})$ [the gradient term in Eq. (6)]. The actual density profile is obtained from condition $\delta\Omega[\rho(\mathbf{r})]/\delta\rho(\mathbf{r})=0$, which gives a variational equation for $\rho(\mathbf{r})$. Using the density profile, the formation free energy is obtained by subtracting the free energy of the supersaturated vapor from Eq. (6). The drawback of SGT is that the local free energy (that is EoS) must be known at all densities, including the unstable regions. In this work we have used the DFT EoS, which is described in Sec. III.

SGT with a parameter fitting has been applied to describe nucleation of LJ fluid,[21] nonane,[22] and polar fluids[23] with some success.

D. DFT

Density functional theory can be considered the most refined of the theories reviewed here. The free-energy is given by[14]

$$\Omega[\rho(\mathbf{r})] = \int d\mathbf{r} f_h(\rho(\mathbf{r})) + \frac{1}{2}\int\int d\mathbf{r}d\mathbf{r}'\,\phi(|\mathbf{r}-\mathbf{r}'|)\rho(\mathbf{r})\rho(\mathbf{r}') - \mu\int d\mathbf{r}\rho(\mathbf{r}). \tag{7}$$

The approach of Eq. (7) is perturbative: a hard-sphere fluid with the free-energy density $f_h(\rho)$ is chosen as a reference system and a perturbation [the second term on the right-hand side of Eq. (7)] is added to account for the attractive interactions. The essential difference between SGT and DFT is that SGT is a purely local theory, whereas in DFT the density at a given point depends on the interactions accounted for over all space, although in Eq. (7) this is done in the mean-field level. For DFT, an interaction potential ϕ must be defined, in our case the LJ potential. The calculation of the density profile and the formation free energy is done as in SGT.

In our earlier study,[21] we showed that DFT with a fitting procedure results in an excellent agreement with MD nucleation simulations of LJ vapors at a relatively low temperature. The same approach was used much earlier by Nyquist *et al.*[24] to nonane and toluene nucleation and considerable improvement over CNT results were found.

The considered theories are all thermodynamic approaches to nucleation which give the formation free energy $\Delta\Omega^*$ of the critical nucleus. The output quantity of MD simulations, however, is the nucleation rate. The relation between the formation energy and the nucleation rate J is

$$J = K\exp(-\Delta\Omega^*/k_BT), \tag{8}$$

where K is a kinetic prefactor. Following Ref. 15, we use the classical formula for K

$$K = v_l\left(\frac{P_v}{k_BT}\right)^2\sqrt{\frac{2\gamma_\infty}{\pi m}}, \tag{9}$$

where m is the molecular mass.

The classical prefactor is only an approximation, but one that works quite well. A MD study[25] of a LJ system showed that when the formation free energy and nucleation rate were obtained from the simulation independently, the simulated formation free energy combined with the classical prefactor gave an accurate estimate of the simulated nucleation rate. In another work, SGT formation free energy and classical prefactor gave only 10% higher nucleation rates than an accurate kinetic calculation.[26] However, a MD analysis of the nucleation kinetics of a LJ system suggested that the classical prefactor can underestimate the numerical value by one order of magnitude.[27]

III. MD DATA SETS AND THERMODYNAMIC CONSISTENCY

The reference MD data set is comprised of three recent nucleation studies in LJ vapors,[6–8] where the actual nucleation event is observed in a simulation box (so-called direct nucleation simulation). All these studies consider a LJ potential that is truncated and shifted at $r_{cut}=2.5\sigma$, where σ is the LJ length parameter. A notable difference exists in the method by which the nucleation rate is extracted from the simulations. Refs. 6 and 8 use the method by Yasuoka and Matsumoto (YM),[28] whereas in Ref. 7 the mean first passage time (MFPT) analysis[29] is applied. In Ref. 8, the simulations are performed in the grand-canonical ensemble and the nucleation rates are shown to agree with those from canonical simulations. The simulations cover temperatures $T=0.65-1.0$, but the data presented at $T=0.95$ and $T=1.0$ are excluded from this study because the reported rates at these temperatures are not probably valid approximations of the actual nucleation rates.[6] Here and throughout the rest of the article, temperatures are scaled with k_B/ϵ, where ϵ is the LJ energy parameter. The critical temperature of the fluid is at $T_c=1.0779$.[30] There exists some uncertainty about the triple point temperature: Ref. 31 gives $T_{tr}=0.65$, whereas in Ref. 32 the value $T_{tr}=0.618$ is reported. In any case, the MD simulations of Refs. 6–8 describe nucleation above the triple point.

The successful application of any nucleation theory requires that the bulk thermodynamic properties used as input are those of the nucleating fluid. Fortunately, simulation-based thermodynamic data are given in Ref. 30 for the particular LJ fluid studied here. The reported properties are the saturated values of pressure and vapor and liquid densities,

surface tension, and the enthalpy of vaporization. The temperature correlations for these quantities given in Ref. 30 are valid for $T=0.64-1.05$, which nicely covers the range of the nucleation simulations.

Nucleation theories also need information on the vapor condition in supersaturated states. If ideal gas is assumed, equilibrium vapor pressure P_e together with the ideal gas law suffice to supply this information, but for a highly nonideal LJ vapor, a realistic EoS should be provided. To our knowledge, there does not exist an EoS for the LJ system truncated and shifted at $r_{\mathrm{cut}}=2.5\sigma$. Using an EoS of the full-potential LJ system and correcting for the cutoff is not recommended when the cutoff value is small.[33] To be fully consistent in the comparison of the theories, we chose the DFT EoS to obtain pressure and chemical potential in all our calculations. DFT EoS is given by the DFT formalism at the limit of homogeneous fluid as

$$P = P_h - \tfrac{1}{2}\alpha\rho^2, \tag{10}$$

where P_h is the hard-sphere pressure according to the Carnahan–Starling formula[34] and $\alpha=-\int d\mathbf{r}\phi(r)$. Knowing the EoS, we describe the state of the vapor in terms of chemical potential rather than density or pressure. Thus, for example, saturation ratio is defined by

$$S = e^{\Delta\mu/k_BT}, \tag{11}$$

where $\Delta\mu$ is the chemical potential difference between the supersaturated and saturated vapor according to the EoS.

The only input the CNT and EMLD-DNT require are surface tension and liquid density in addition to EoS. The latent heat of vaporization needed in DIT were obtained from Ref. 30. It should be kept in mind that in CNT and DIT, $\Delta\mu$ is an external parameter (the "μ form" of CNT in Ref. 35) and EoS does not directly enter to the calculation, whereas EMLD-DNT uses the actual EoS.

While CNT, DIT, and EMLD-DNT are purely theories of nucleation, SGT and DFT are more general theories of fluid state which can be applied in the planar geometry as well. They thus provide surface tension, which depends on the parameter c (SGT) or the potential parameters (DFT). As in our earlier paper,[21] the parameter c in SGT was fitted to give the MD surface tension. The free parameters in DFT are the two LJ parameters (σ and ϵ) and the hard-sphere diameter (d). These were fitted to give the MD values of P_e, ρ_l, and γ_∞ at each studied temperature and the DFT EoS with the same parameters were also used in the other theories. In the temperature range $T=0.65-0.9$ we obtain $\sigma'/\sigma=1.031-1.064$, $\epsilon'/\epsilon=0.996-1.006$, and $d'/d=1.026-1.027$, where the primed quantities denote the new set of parameters.

To correlate the vapor densities in MD simulations of Ref. 7 with the corresponding chemical potential differences $\Delta\mu$, we used at $T=0.65$ and $T=0.8$ the same simulated pressure-vapor density correlations as in Ref. 7. This EoS was also applied to convert the pressure ratios P_v/P_e reported in Ref. 6 to chemical potential differences (temperatures 0.65 and 0.8). Finally, the saturation ratios given in Ref. 8 were used as such to calculate $\Delta\mu$ according to Eq. (11).

The use of consistent set of bulk thermodynamic parameters, the same EoS, and, if necessary, a fitting procedure sets the theories on equal footing: they are all identical at the bulk level (at least as far as input data for nucleation is concerned) and thus the differences in calculated nucleation rates better reflect the true differences between the theories.

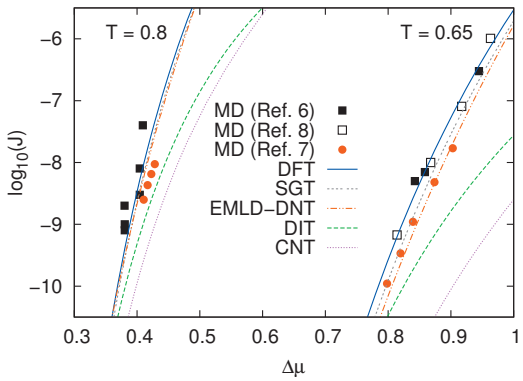

FIG. 1. Nucleation rates for a LJ fluid truncated and shifted at 2.5σ as function of the chemical potential difference between supersaturated and saturated vapors. Shown are results from MD simulations and theoretical calculations. Temperatures are given in units of ϵ/k_B and chemical potential in units of ϵ.

IV. RESULTS AND DISCUSSION

A. Nucleation rate

Logarithmic nucleation rates as a function of $\Delta\mu=k_BT\ln S$ are depicted in Fig. 1 at $T=0.65$ and $T=0.8$. The figure shows the MD nucleation rate data[6–8] together with nucleation rates from the theories reviewed in Sec. II, including CNT. There is a small difference between the MD data sets at $T=0.65$ and the difference increases up to one order of magnitude at $T=0.8$, although at the latter temperature the scatter in the data of Ref. 6 makes it difficult to evaluate the exact deviation. It seems that the simulations using the YM method yield somewhat higher nucleation rates than those using the MFPT method. Chkonia *et al.*[36] have shown that these methods should result in similar nucleation rates; the conclusions, however, were based on simulations at the triple point temperature and in the present study we are above it (at $T=0.65$, the difference between the methods is almost negligible). Whether there really is a methodological difference or the source for the discrepancy lies elsewhere remains unclear (see also Ref. 37). We do not pursue the matter further here.

According to Fig. 1, the MD nucleation rates are reproduced with good accuracy by DFT, SGT, and EMLD-DNT. At $T=0.8$, the nucleation rates from these theories practically coincide. DIT underestimates the MD rates, especially at $T=0.65$. Not unexpectedly, CNT gives the worst results. The overall deviation of the theoretical nucleation rates from the MD data is less than one order of magnitude, excluding CNT and DIT.

Figure 1 shows that the difference between the simulated nucleation rates J_{MD} and theoretical nucleation rates J_{theor} depends on the saturation ratio somewhat. Regardless, it is worthwhile to consider a situation where this dependence is ignored and to investigate the performance of the theories at different temperatures by plotting the ratios $\log_{10}(J_{\mathrm{MD}}/J_{\mathrm{theor}})$

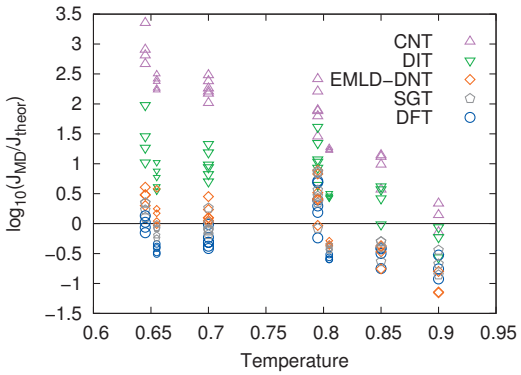

FIG. 2. The logarithmic ratios of simulated and theoretical nucleation rates at different temperatures. The larger symbols refer to simulations of Refs. 6 and 8 and the smaller symbols to the simulations of Ref. 7.

at each studied temperature, although some scatter in the vertical direction ensues. Such a plot is shown in Fig. 2. The larger symbols relate to simulations of Refs. 6 and 8 and the smaller symbols to the simulations of Ref. 7. Again we see that DFT, SGT, and EMLD-DNT manage best in predicting the MD results with the nucleation rate always within one order of magnitude from the simulated one. EMLD-DNT, however, shows a little more deviation than DFT and SGT. DIT, which on the basis of Fig. 1 showed considerable deviation at $T=0.65$, actually fares much better at higher temperatures. At $T=0.9$, CNT seems to indicate an almost perfect match between theory and simulation, but experiments show that there is usually one temperature where the nucleation rates from CNT intersect the experimental ones.[38]

The main trend in Fig. 2 seems to be that for all theories, $\log_{10}(J_{\mathrm{MD}}/J_{\mathrm{theor}})$ decreases with increasing temperature; in other words, the theoretical nucleation rate increases with respect to the simulated rate. Only at $T=0.8$ the ratios shown as large symbols are somewhat elevated; this may be a real effect or an artifact caused by incompatibility of the MD EoS of Ref. 7 with the pressure data of Ref. 6

Kalikmanov *et al.*[15] compared mean-field kinetic nucleation theory and EMLD-DNT to MD simulations of Refs. 39 and 18 and to DFT calculations of Ref. 14. Our Fig. 2 should be compared with Fig. 2 of Ref. 15. In accordance with our results, Kalikmanov *et al.* found that EMLD-DNT closely predicts the MD nucleation rates. However, the DFT rates in Ref. 15 are three to four orders of magnitude higher than EMLD-DNT rates, whereas our calculations show that the EMLD-DNT and DFT rates differ less than one order of magnitude. The likely reason for this discrepancy is that in Ref. 15 the DFT data of Ref. 14 were used without any parameter fitting to the bulk data.

B. Critical cluster size

There is some interest to appraise the critical cluster sizes from theoretical approaches. The comparison to simulations is not straightforward because the critical cluster size is not a uniquely defined quantity. There exist cluster definitions based on the thermodynamics of surfaces, geometric definitions, and energetic rules. The most generally applicable definition is given by the nucleation theorem (NT),[40] which gives the excess number of particles in the critical cluster as

$$\Delta N^* \approx k_B T \frac{\partial \ln J}{\partial \Delta\mu} - 1. \tag{12}$$

Only the nucleation rate data are required to calculate the NT size of the cluster in a given vapor. The uncertainty in ΔN^* in Eq. (12) is about one particle.

The cluster definition based on Eq. (12) is adopted in this study. To obtain the cluster sizes from the simulation data, we have fitted the MD nucleation rates at each temperature to a simple CNT-like function $\ln J=a(T)(\Delta\mu)^{-2}+b(T)$, which, partly owing to the narrow range of MD data in the $\Delta\mu$ space, gives a good estimate of the actual nucleation rates. Note, however, that a cluster definition is already needed to obtain the MD nucleation rates from MFPT analysis and NT cannot be used for this purpose. We have reported nucleation rates according to the Stillinger definition[41] and the ten Wolde–Frenkel (TWF)[42] definition in our previous paper.[7] The two cluster definitions yield practically the same nucleation rates, but a slight difference in $\Delta\mu$-dependence of the nucleation rate curves causes a noticeable change in the cluster sizes. The TWF-based rates are used in this paper. Applying the Stillinger definition in MFPT analysis instead of the TWF definition decreases the NT cluster sizes 2.3% at $T=0.65$ and 4.3% at $T=0.8$.

In EMLD-DNT and DIT the critical cluster sizes are obtained via NT by calculating numerical derivatives of the nucleation rate data. DFT and SGT give the excess number of particles in the cluster as an integrated quantity from the density profile, but this quantity agrees with NT.

Figure 3 shows the critical cluster sizes according to the theories and simulations at $T=0.65$, $T=0.7$, and $T=0.8$. For comparison, we also show CNT values and the particle number excesses obtained from the cluster-vapor equilibrium simulations of our previous study.[7] DFT seems to give the best theoretical results, although at $T=0.8$ the sizes are overestimated. DFT is closely matched by SGT with only slightly larger sizes. CNT and especially DIT underestimate the MD sizes and EMLD-DNT, in the range of supersaturations of the MD data sets, overestimates them. We note that due to the scatter in the MD data of Ref. 6 at $T=0.8$, the fitting of the nucleation rate and resulting cluster sizes are unreliable.

The EMLD-DNT sizes are too large at higher saturation ratios and the dependence of size on $(\Delta\mu)^{-3}$ is clearly wrong. While EMLD-DNT predicts MD nucleation rates quite well according to Fig. 1, the slopes of the EMLD-DNT nucleation rate curves are slightly different from DFT, SGT, and MD curves, which produces a considerable effect in Fig. 3 when NT is used to calculate the cluster sizes. At lower saturation ratios, where no MD simulations are available, the EMLD-DNT sizes approach the CNT line. The problems of EMLD-DNT at high saturation ratios have already been addressed by Reguera and Reiss in Ref. 11. The pressure of the vapor in the small container in EMLD-DNT does not correspond to that given by EoS, which distorts the relation between P_{min} and V_{min}.

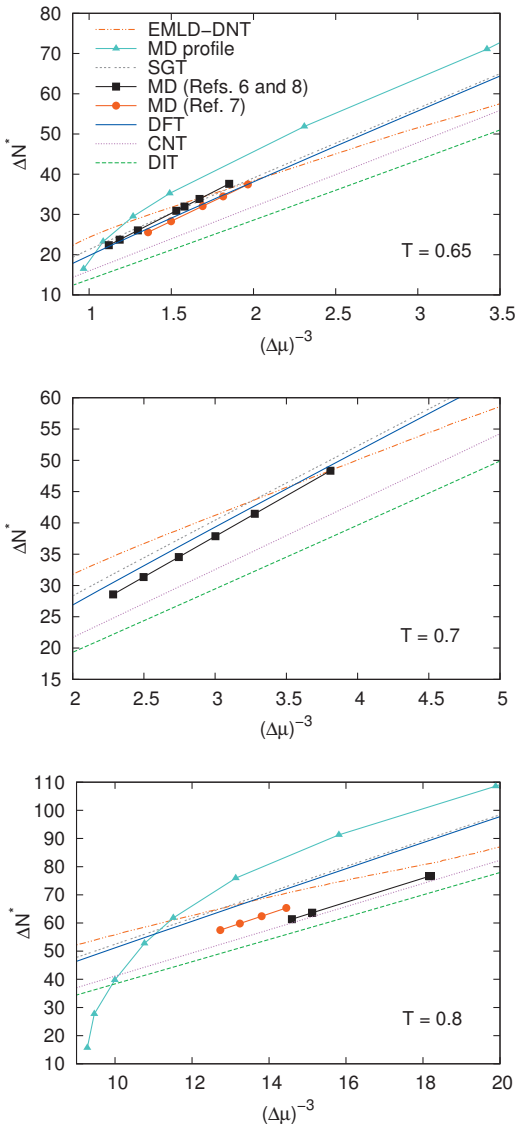

FIG. 3. The theoretical and simulated excess number of particles in the critical cluster at $T=0.65$, $T=0.7$, and $T=0.8$. The MD sizes are based on fitting the nucleation rate data of Refs. 6–8 and using the nucleation theorem. The MD profile size is obtained from the cluster-vapor equilibrium profiles of Ref. 7.

C. Effect of equation of state

We have used DFT EoS to achieve consistency between the nucleation theories in metastable vapor states. However, in SGT and EMLD-DNT one is free to choose any EoS. In our earlier work[21] we used Peng–Robinson (PR) EoS (Ref. 43) to calculate SGT rates. Motivated by the apparent success of SGT in that paper, we have also performed the SGT and EMLD-DNT calculations with PR EoS.

Resembling van der Waals EoS, PR EoS is a two-parameter model. We fitted the parameters to reproduce the MD equilibrium vapor pressure and liquid density. The resulting EoS gives a better approximation of the correlation between the density and pressure of the metastable LJ vapor than DFT EoS, which overestimates the pressure. However, the calculated nucleation rates deviate more from the MD values than the rates obtained using DFT EoS: compared to the results presented in Figs. 1 and 2, the SGT rates increase one to two orders of magnitude and the EMLD-DNT one order of magnitude at high supersaturations. EMLD-DNT nucleation rates are close to MD rates at the lower end of the vapor density range, but the slope of the nucleation rate curves is erroneous. When NT is used, the wrong slope translates to much larger cluster sizes than those shown in Fig. 3. The SGT sizes are also somewhat larger.

PR EoS also causes a problem in EMLD-DNT calculations. At high saturation ratios, there may not be a minimum on a $P(V)$ curve, even though a (hypothetical) small-system EoS would indicate otherwise. In this study, we did not find the critical cluster at high saturation ratios at $T=0.85$ and $T=0.9$ when PR EoS was used.

V. CONCLUSIONS

We have performed an assessment of several nucleation theories by comparing the calculated nucleation rates and critical cluster sizes to MD simulation values in the nucleation of LJ vapors. The comparison has been done so that the theories either use or predict the same bulk thermodynamic properties as MD. Realistic EoS has been used to account for the nonideality of the vapor. The studied temperatures are above the triple point of the LJ fluid and the saturation ratios correspond to vapor conditions where the nucleation rates are high.

Our results support the previous results on LJ nucleation[11,15,18,21] and they also seem to be in accordance with the studies where the theories were compared to real nucleation experiments,[9,19,24] with the possible exception of SGT.[22,23] It is therefore justified to draw general conclusions based on the results of this study.

The best results are obtained from DFT, which reproduces both the MD nucleation rates and critical cluster sizes rather well. DFT is unfortunately limited to rather simple fluids, where the intermolecular interactions can be described by a spherically symmetric potentials unless a more complicated version of the theory, such as interaction site model,[44] is applied. SGT does not need an interaction potential and the SGT nucleation rates and cluster sizes are close to DFT values. Unfortunately, SGT is quite sensitive to the choice of EoS. DIT somewhat underestimates the nucleation rate, but it is still much better than CNT when predicting nucleation rates. DIT is easy to use because it is almost as simple as CNT and needs only the heat of evaporation as an additional input, but its applicability to polar substances is questionable.[9] EMLD-DNT almost equals DFT in predicting nucleation rates, but the dependence of the nucleation rate on saturation ratio is slightly wrong, which results in erroneous cluster sizes. This problem arises at high vapor densities, where EMLD-DNT is also highly dependent on EoS. EMLD-DNT is thus at its best when applied to nearly ideal vapors.

ACKNOWLEDGMENTS

This research was supported by the Academy of Finland Center of Excellence program (Project No. 1118615).

[1] L. Farkas, Z. Phys. Chem., Stoechiom. Verwandtschaftsl. **125**, 236 (1927).
[2] J. Feder, K. C. Russell, J. Lothe, and G. M. Pound, Adv. Phys. **15**, 111 (1966).
[3] I. J. Ford, J. Mech. Eng. Sci. **218**, 883 (2004).
[4] D. Brus, A. P. Hyvärinen, and V. Zdimal, J. Chem. Phys. **122**, 214506 (2005).
[5] E. Herrmann, A. P. Hyvärinen, D. Brus, H. Lihavainen, and M. Kulmala, J. Phys. Chem. A **113**, 1434 (2009).
[6] M. Horsch, J. Vrabec, and H. Hasse, Phys. Rev. E **78**, 011603 (2008).
[7] I. Napari, J. Julin, and H. Vehkamäki, J. Chem. Phys. **131**, 244511 (2009).
[8] M. Horsch and J. Vrabec, J. Chem. Phys. **131**, 184104 (2009).
[9] L. Gránásy, J. Chem. Phys. **104**, 5188 (1996).
[10] D. Reguera and H. Reiss, Phys. Rev. Lett. **93**, 165701 (2004).
[11] D. Reguera and H. Reiss, J. Phys. Chem. B **108**, 19831 (2004).
[12] J. W. Cahn and J. E. Hilliard, J. Chem. Phys. **28**, 258 (1958).
[13] J. W. Cahn and J. E. Hilliard, J. Chem. Phys. **31**, 688 (1959).
[14] X. C. Zeng and D. W. Oxtoby, J. Chem. Phys. **94**, 4472 (1991).
[15] V. I. Kalikmanov, J. Wölk, and T. Kraska, J. Chem. Phys. **128**, 124506 (2008).
[16] D. Reguera, R. K. Bowles, Y. Djikaev, and H. Reiss, J. Chem. Phys. **118**, 340 (2003).
[17] D. Reguera and H. Reiss, J. Chem. Phys. **119**, 1533 (2003).
[18] J. Wedekind, J. Wölk, D. Reguera, and R. Strey, J. Chem. Phys. **127**, 154515 (2007).
[19] R. Zandi, D. Reguera, and H. Reiss, J. Phys. Chem. B **110**, 22251 (2006).
[20] J. D. van der Waals, Verh. K. Akad. Wet. Amsterdam, Afd. Natuurkd. **1**, 56 (1893).
[21] J. Julin, I. Napari, J. Merikanto, and H. Vehkamäki, J. Chem. Phys. **129**, 234506 (2008).
[22] J. C. Barrett, J. Phys.: Condens. Matter **9**, L19 (1997).
[23] A. Obeidat and G. Wilemski, Atmos. Res. **82**, 481 (2006).
[24] R. M. Nyquist, V. Talanquer, and D. W. Oxtoby, J. Chem. Phys. **103**, 1175 (1995).
[25] J. Wedekind, G. Chkonia, J. Wölk, R. Strey, and D. Reguera, J. Chem. Phys. **131**, 114506 (2009).
[26] J. Hrubý, D. G. Labetski, and M. E. H. van Dongen, J. Chem. Phys. **127**, 164720 (2007).
[27] P. R. ten Wolde, M. J. Ruiz-Montero, and D. Frenkel, J. Chem. Phys. **110**, 1591 (1999).
[28] K. Yasuoka and M. Matsumoto, J. Chem. Phys. **109**, 8451 (1998).
[29] J. Wedekind, R. Strey, and D. Reguera, J. Chem. Phys. **126**, 134103 (2007).
[30] J. Vrabec, G. K. Kedia, G. Fuchs, and H. Hasse, Mol. Phys. **104**, 1509 (2006).
[31] J. A. van Meel, A. J. Page, R. P. Sear, and D. Frenkel, J. Chem. Phys. **129**, 204505 (2008).
[32] S. Toxvaerd, J. Phys. Chem. C **111**, 15620 (2007).
[33] V. G. Baidakov and S. P. Protsenko, High Temp. **41**, 195 (2003).
[34] N. F. Carnahan and K. E. Starling, J. Chem. Phys. **51**, 635 (1969).
[35] A. Obeidat, J.-S. Li, and G. Wilemski, J. Chem. Phys. **121**, 9510 (2004).
[36] G. Chkonia, J. Wölk, R. Strey, J. Wedekind, and D. Reguera, J. Chem. Phys. **130**, 064505 (2009).
[37] F. Römer and T. Kraska, J. Chem. Phys. **127**, 234509 (2007).
[38] J. Wölk, R. Strey, C. H. Heath, and B. E. Wyslouzil, J. Chem. Phys. **117**, 4954 (2002).
[39] T. Kraska, J. Chem. Phys. **124**, 054507 (2006).
[40] D. Kashchiev, J. Chem. Phys. **76**, 5098 (1982).
[41] F. H. Stillinger, J. Chem. Phys. **38**, 1486 (1963).
[42] P. R. ten Wolde and D. Frenkel, J. Chem. Phys. **109**, 9901 (1998).
[43] D.-Y. Peng and D. B. Robinson, Ind. Eng. Chem. Fundam. **15**, 59 (1976).
[44] V. Talanquer and D. W. Oxtoby, J. Chem. Phys. **103**, 3686 (1995).